EXPERIMENTAL and MOLECULAR MEDICINE, Vol. 44, No. 8, 503-512, August 2012

Genome-scale DNA methylation pattern profiling of human bone marrow mesenchymal stem cells in long-term culture

Mi Ran Choi[1]*, Yong-Ho In[2]*, Jungsun Park[2,3], Taesung Park[3,4], Kyoung Hwa Jung[1], Jin Choul Chai[1], Mi Kyung Chung[5], Young Seek Lee[1] and Young Gyu Chai[1,6]

[1]Department of Molecular and Life Sciences
Hanyang University
Ansan 426-791, Korea
[2]Medicinal Bioconvergence Research Center
Seoul National University
Suwon 443-270, Korea
[3]Interdisciplinary Program in Bioinformatics
[4]Department of Statistics
Seoul National University
Seoul 151-747, Korea
[5]Fertility Center
CHA Gangnam Medical Center
CHA University
Seoul 135-081, Korea
[6]Corresponding author: Tel, 82-31-400-5513;
Fax, 82-31-406-6316; E-mail, ygchai@hanyang.ac.kr
*These authors contributed equally to this work.
http://dx.doi.org/10.3858/emm.2012.44.8.057

Accepted 5 June 2012
Available Online 8 June 2012

Abbreviations: BM, bone marrow; BP, biological processes; DAVID, Database for Annotation, Visualization and Integrated Discovery; HCPs, high CpG promoters; HEFs, human embryonic lung fibroblasts; ICPs, intermediate CpG promoters; IEF, immunoaffinity-enriched DNA fragments; KEGG, Kyoto Encyclopedia of Genes and Genomes; LCPs, low CpG promoters; MeDIP, methylated DNA immunoprecipitation; miRNAs, microRNAs; MSCs, mesenchymal stem cells; MSP, methylation-specific PCR; P, passage

Abstract

Human bone marrow mesenchymal stem cells (MSCs) expanded *in vitro* exhibit not only a tendency to lose their proliferative potential, homing ability and telomere length but also genetic or epigenetic modifications, resulting in senescence. We compared differential methylation patterns of genes and miRNAs between early-passage [passage 5 (P5)] and late-passage (P15) cells and estimated the relationship between senescence and DNA methylation patterns. When we examined hypermethylated genes (methylation peak $\geq$ 2) at P5 or P15, 2,739 genes, including those related to fructose and mannose metabolism and calcium signaling pathways, and 2,587 genes, including those related to DNA replication, cell cycle and the PPAR signaling pathway, were hypermethylated at P5 and P15, respectively. There was common hypermethylation of 1,205 genes at both P5 and P15. In addition, genes that were hypermethylated at P5 (CPEB1, GMPPA, CDKN1A, TBX2, SMAD9 and MCM2) showed lower mRNA expression than did those hypermethylated at P15, whereas genes that were hypermethylated at P15 (MAML2, FEN1 and CDK4) showed lower mRNA expression than did those that were hypermethylated at P5, demonstrating that hypermethylation at DNA promoter regions inhibited gene expression and that hypomethylation increased gene expression. In the case of hypermethylation on miRNA, 27 miRNAs were hypermethylated at P5, whereas 44 miRNAs were hypermethylated at P15. These results show that hypermethylation increases at genes related to DNA replication, cell cycle and adipogenic differentiation due to long-term culture, which may in part affect MSC senescence.

Keywords: cell cycle; DNA methylation; DNA replication; gene expression profiling; mesenchymal stem cells; microRNAs

Introduction

Mesenchymal stem cells (MSCs) can be easily isolated, adhere proficiently to plastic and self-renew; they are considered to have great therapeutic potential. However, because they exist at low frequencies (0.01% to 0.001%) in bone marrow (BM) (Choi *et al*., 2010), it is necessary to expand MSCs *ex vivo* prior to clinical use. Previous studies have demonstrated that MSCs expanded *in vitro* exhibit a tendency to lose their proliferative potential, homing ability, capability to secrete cytokines, and,

ultimately, undergo senescence (Bruder *et al*., 1997; Rombouts and Ploemacher, 2003; Choi *et al*., 2010). Meanwhile, some studies have reported that long-term MSC cultures displayed not only the shortening of telomeres and the absence of telomerase expression and activity (Baxter *et al*., 2004; Bernardo *et al*., 2007; Choi *et al*., 2010) but also genetic or epigenetic modifications, contributing to cellular senescence (Dahl *et al*., 2008; Bork *et al*., 2010).

Expression of mammalian genes can be regulated by epigenetic processes, including DNA methylation, chromatin remodeling and the noncoding RNA-mediated mechanism (Bird, 2002). DNA methylation, which is the methylation of cytosines in CpG dinucleotides, favors genomic integrity and thus properly regulates gene expression (Antequera, 2003). Recently, some studies have analyzed methylation patterns of MSCs during long-term culture or differentiation and have suggested the possibility of epigenetic instability due to long-term culture as well as changes in gene methylation due to differentiation (Noer *et al*., 2006; Dahl *et al*., 2008; Bork *et al*., 2010). Bork *et al*. (2010) reported that highly significant differences in methylation patterns were observed at specific CpG sites, such as those near homeobox genes between early and late cultures. Meanwhile, using human embryonic lung fibroblasts (HEFs), Zhang *et al*. (2008) compared DNA methylation globally with respect to replicative versus premature senescence induced by hydrogen peroxide. They reported that genome methylation levels decreased gradually, suggesting that changes in methylation might be partly responsible for cellular senescence.

MicroRNAs (miRNAs), which are small (~22-nucleotide) noncoding RNA molecules that regulate the expression of genes related to the development, differentiation and proliferation of stem cells through complex regulatory networks (Hammond and Sharpless, 2008; Godlewski *et al*., 2010; Schaefer *et al*., 2010). Wagner *et al*. (2008) demonstrated that miRNAs, including has-mir-371, were up-regulated upon replicative senescence of MSCs, showing that senescence influences the expression of miRNAs. It has been reported that the expression of miRNAs may be regulated by the methylation of miRNA promoters (Liang *et al*., 2009). In addition, the methylation status of miRNA promoters may be indirectly associated with miRNA-directed post-transcriptional regulation of other factors, such as those in the methyltransferase family (Sinkkonen *et al*., 2008). Taken together, it is worth considering the relationship between methylation of miRNA promoters and expression of miRNAs upon replicative senescence of MSCs.

In the present study, we measured the telomere shortening of human BM-derived MSCs as a result of long-term culture. We performed methylated DNA immunoprecipitation (MeDIP) assays and combined them with gene expression microarrays to compare differential methylation patterns of DNA and miRNA promoters between early (passage 5; P5) and late (passage 15; P15) passage cells. We also attempted to estimate the association between MSC senescence and DNA methylation patterns.

Results

Telomere shortening in long-term culture

Telomere shortening after each division cycle leads to gradual senescence. To evaluate telomere shortening, we measured the relative telomere length of MSCs at P5, P7, P9, P12 and P15 by the standard curve method (Figures 1A and 1B). T/S ratios, which indicate relative telomere length, of the cells continuously decreased from 2.85 at P5 to 1.6 at P15 and T/S ratios at P5 exhibited significant difference from these at P12 and P15 (Figure 1C). Applying a conversion factor (Cawthon, 2002) to convert T/S ratios into their corresponding mean TRF length at P5, P7, P9, P12 and P15 were 9.6, 9, 8.5, 8.2 and 7.2 kb, respectively; this results in shortening of the telomeres by 2.4 kb from P5 to P15.

Validation of MeDIP

To validate input and immunoaffinity-enriched DNA fragments (IEF) DNA from MSCs at P5 and P15, we amplified the *GPR109A*, *SFRS5* and *PEX13* promoters from the input and IEF using PCR as previously described (Weber *et al*., 2007). A band corresponding to the *GPR109A* promoter was detected in both the input and IEF samples at P5 and P15 (Figure 2). The band representing the *SFRS5* promoter was much stronger in the input sample than that of IEF at P5 and P15. The patterns of these three promoters are in agreement with those reported by Weber *et al*. (2007), who demonstrated the successful enrichment of methylated DNA using MeDIP methodology. Therefore, the enrichment of methylated DNA in the MeDIP procedure was properly accomplished.

Profiling of promoter DNA methylation and miRNA methylation

To compare differential promoter methylation patterns between P5 and P15 MSCs, we performed DNA methylation microarrays using NimbleGen human

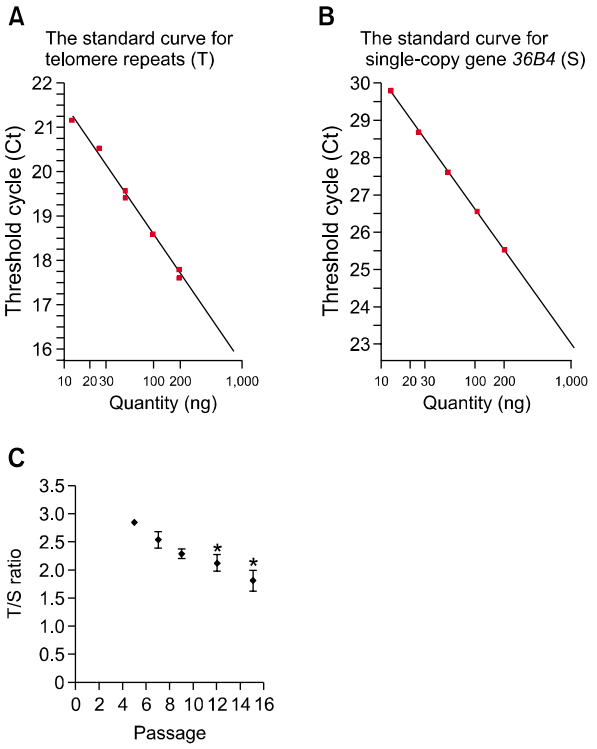

Figure 1. Relative telomere length expressed as the T/S ratio. Using quantitative real-time PCR, relative telomere length of genomic DNAs from MSCs at various passages (P) (i.e., P5, P7, P9, P12 and P15) were calculated compared with human embryonic carcinoma NCCIT cells (reference). (A) The standard curve for telomere repeats (T). (B) The standard curve for the single-copy gene *36B4* (S). The standard curves for T and S were obtained from serial dilutions of genomic DNA (200 ng to 12.5 ng) from NCCIT cells (telomerase-positive cell line). (C) T/S ratios of MSCs obtained at P5, P7, P9, P12 and P15. T/S ratios indicate the relative telomere length and are represented as the mean ± SEM (n = 3) from three independent experiments. *Significantly different from P5 by a one-way ANOVA, followed by Tukey's HSD post hoc test (*$P < 0.05$).

2.1 M Deluxe Promoter Arrays. This array covers 10 kb of the promoter region for all known genes, including those near alternative transcription start sites. When we analyzed the methylation differences between P5 and P15, 3,338 genes showed more than two-fold higher methylation at P5 than P15, whereas 4,670 genes showed more than two-fold higher methylation at P15 than P5 (Figure 3A). Among 3,338 genes with higher methylation at P5, 2,867 (85.9%) were methylated at low CpG promoters (LCPs), and 471 (14.1%) were methylated at intermediate CpG promoters (ICPs); there were no genes at high CpG promoters (HCPs) (Figure 3B). In case of genes with higher methylation at P15, 4,026 (86.2%) were methylated at LCPs, and 644 (13.8%) were methylated at ICPs; again, there were no genes at HCPs.

When we further analyzed genes exhibiting hypermethylated promoters (methylation peak ≥ 2)

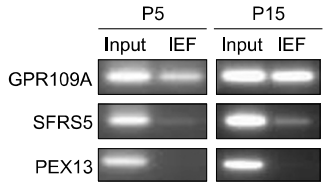

Figure 2. Validation of methyl-DNA immunoprecipitation (MeDIP). Genomic DNA from MSCs at P5 and P15 was sonicated and immunoprecipitated with 5-methylcytidine mAb. Validation of immunoaffinity-enriched DNA fragments (IEF) was performed using PCR. Input is the sonicated fragment.

at P5 and P15, 2,739 genes were hypermethylated at P5, and 2,587 genes were hypermethylated at P15. The hypermethylation of 1,205 genes was shared between P5 and P15 (Figure 4). In the case of hypermethylated miRNAs (methylation peak ≥ 2), 27 miRNAs, including has-mir-136, has-mir-150, has-mir-200c and has-mir-618, were hypermethylated at P5, while 44 miRNAs, including has-let-7e, has-mir-27b, has-mir-411 and has-mir-195, were hypermethylated at P15 (Supplemental Data Figure S1). However, in the case of MSCs, most miRNAs hypermethylated at P5 and P15 have yet to be reported in epigenetic modification or gene expression.

Gene ontology and pathway analysis

To identify the biological processes (BP) of genes that showed methylation differences between P5 and P15, GO annotation (annotation category: GOTERM_BP_FAT) was performed using the Database for Annotation, Visualization and Integrated Discovery (DAVID) functional annotation tool. Genes related to biological adhesion (GO:0022610) and cell adhesion (GO:0007155) were methylated at P5 more than twice as compared to P15 (Supplemental Data Table S1). Genes related to cell migration (GO:0016477), cell morphogenesis involved in differentiation (GO:0000904) and Wnt receptor signaling pathway through beta-catenin (GO:0060070) were methylated at P15 more than twice as compared to P5 (Supplemental Data Table S2). Promoters determined to be hypermethylated (methylation peak ≥ 2) at P5 and P15 were also classified with GO annotation (annotation category: GOTERM_BP_FAT). Of the 1,534 genes hypermethylated only at P5, more than 160 genes were commonly involved in phosphate metabolic process (GO:0006796) and cell adhesion (GO:0007155) (Figure 4) (Supplemental Data Table S3). Of the 1,382 genes hypermethylated only at P15, 175 genes were commonly involved in ion transport (GO:0006811), transmembrane transport (GO:

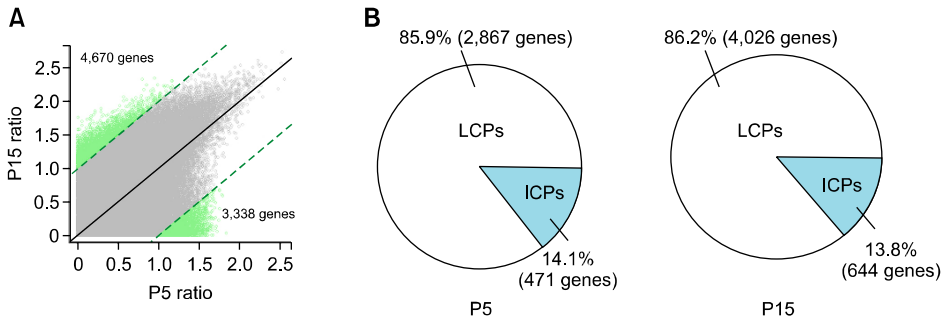

Figure 3. Frequency of DNA methylation in promoter classes. DNA methylation profiling was performed using MSCs at P5 and P15. (A) The scatter plot shows DNA methylation levels for all promoters. Each point represents one promoter, and the green points represent promoters methylated more than two-fold at between P5 and P15. (B) Pie charts showing the frequency of classes (i.e., HCPs, ICPs and LCPs) were classified *via* data obtained from (A). There were no HCPs, which indicate a difference in DNA methylation that occurred more than twice of P5 and P15 (For interpretation of the references to color in this figure legend, the reader is referred to the web version of the article).

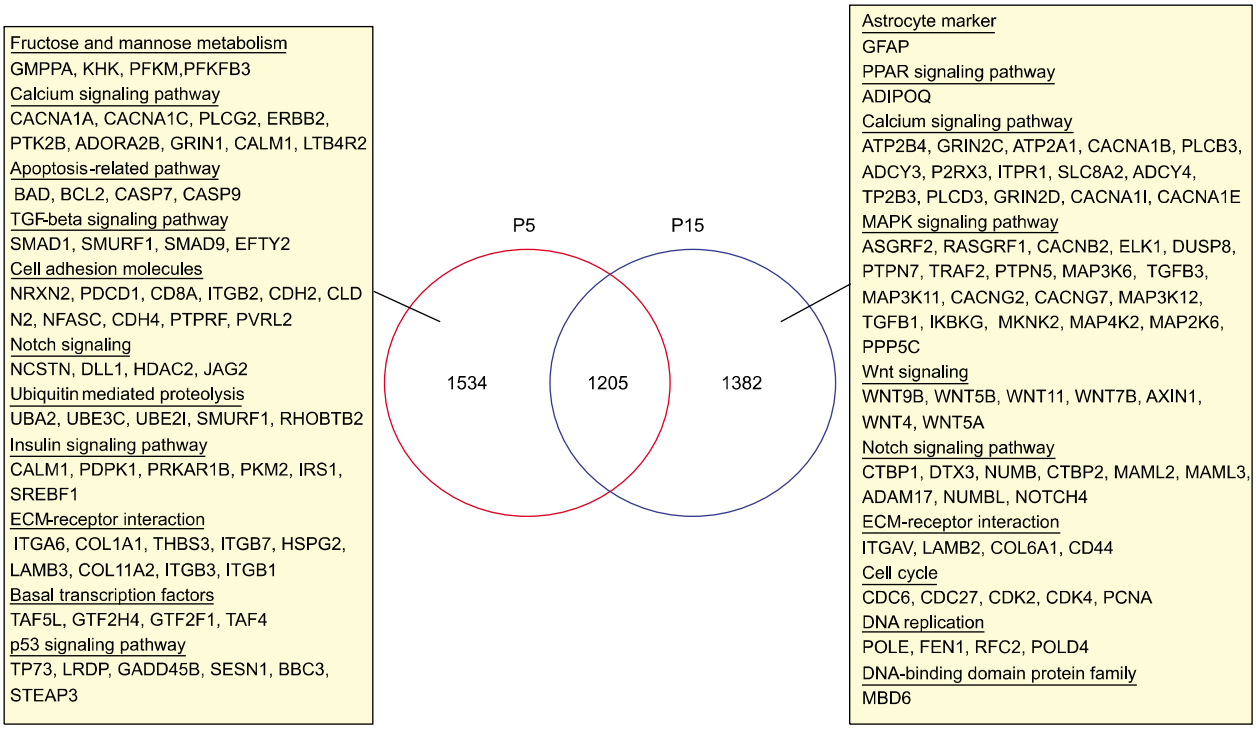

Figure 4. Combination of hypermethylated genes and the summarized KEGG pathway. After sorting the genes hypermethylated (methylation peak $\geq$ 2) at P5 and P15 in MSCs, the data were classified using KEGG pathway analysis. Venn diagrams show hypermethylated genes at P5 and P15, including the overlap between P5 and P15.

0055085) and neuron differentiation (GO:0030182) (Figure 4) (Supplemental Data Table S4).

To further examine potentially disrupted pathways due to hypermethylation, the Kyoto Encyclopedia of Genes and Genomes (KEGG) database was used. Genes related to fructose and mannose metabolism (GMPPA, KHK and so on), the calcium signaling pathway (CACNA1A, CALM1, etc.) and ubiquitin mediated proteolysis (UBA2, UBE3C, UBE2I, etc.) were mainly hypermethylated at P5, whereas genes related to DNA replication (POLE, FEN1, RFC2 and POLD4), cell cycle (CDC6, CDC27, CDK2 and so on), the MAPK signaling pathway (MAP3K6, MAP3K11, MAP4K2 and so on), astrocyte differentiation (GFAP) and target of the PPAR signaling pathway (ADIPOQ) were mainly hypermethylated at P15 (Figure 4). Comparing the hypermethylation of WNT subtypes between P5 and P15, most WNT subtypes (i.e., WNT4, WNT5A, WNT5B, WNT7B, WNT9B and WNT11) except WNT10A were specifically

hypermethylated at P15, showing the possibility that the Wnt signaling pathway, which regulates cell fate, adhesion and migration (Nelson and Nusse, 2004), is down-regulated in late-passage MSCs, compared with early-passage MSCs.

Validation of differentially methylated genes

Differential methylation of promoters in CPEB1, TBX2 and SMAD9 genes was validated by semi-quantitative methylation-specific PCR (MSP) after bisulfite modification. Based on the results obtained from DNA methylation microarrays, MSP primers were designed within sequences from peak start site to peak end site of methylation in gene promoter. Methylation density of CPEB1 and SMAD9 at P5 was greatly higher than unmethylation density of these genes, while unmethylation density of CPEB1 and SMAD9 at P15 increased compared to P5 (Figure 5A), showing the same pattern as DNA methylation microarray analysis (Figure 5B). On the other hand, methylation or unmethylation density of TBX2 at P5 was not changed at P15. This result is likely by examining a part sequence within promoter showing hypermethylated signal in DNA methylation microarray.

Correlation of DNA methylation and gene expression

It has been generally known that DNA methylation represses gene expression. To analyze the correlation between DNA promoter methylation and gene expression, we observed mRNA expression of CPEB1, GMPPA, CDKN1A, TBX2, SMAD9, MCM2, MAML2, FEN1 and CDK4 genes in MSCs at P5 and P15. Genes (i.e., CPEB1, GMPPA, CDKN1A, TBX2, SMAD9 and MCM2) hypermethylated at P5 showed lower mRNA expression at P5 than at P15, whereas genes (i.e., MAML2, FEN1 and CDK4) hypermethylated at P15 showed lower mRNA expression at P15 than at P5 (Figures 5A and 5B). For these genes, hypermethylation at DNA promoter regions inhibited gene expression.

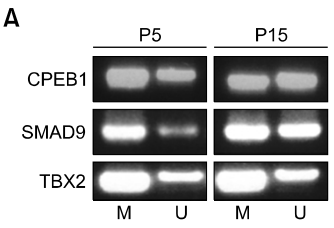

B

Gene	P5	P15
CPEB1	2.59	-
GMPPA	2.42	-
CDKN1A	2.58	-
SMAD9	2.27	-
TBX2	2.35	-
MCM2	2.60	-
MAML2	-	2.66
FEN1	-	2.59
CDK4	-	2.53

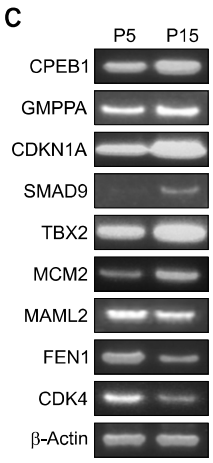

Figure 5. Correlation between DNA methylation and mRNA expression of MSCs. To evaluate DNA methyation and mRNA expression, MSCs harvested at P5 and P15 were used. (A) Methylation-specific PCR was performed using bisulfite-modified genomic DNA at P5 and P15. M, methylated product; U, unmethylated product. (B) DNA methylation was analyzed using NimbleGen human 2.1M Deluxe Promoter Array (NimbleGen). The value of each gene at P5 and P15 shows the ratio of immunoaffinity-enriched DNA fragments (IEF)/input, methylation intensity. The value of more than two means the hypermethylation of the gene. The value of low methylated or little methylated genes was not described. Input is the sonicated DNA fragment. (C) mRNA expression changes in MSCs at P5 and P15 were measured using RT-PCR.

Discussion

The potential of proliferation and differentiation in adult stem cells obtained from various tissues is decreased during *in vitro* long-term culture, inducing their senescence. It has been reported that various mechanisms such as telomere shortening, histone modification, DNA methylation and miRNA expression affect the proliferation and differentiation of MSCs, resulting in cell senescence (Bonab *et al*., 2006; Noer *et al*., 2006; Wagner *et al*., 2008; Zhang *et al*., 2008; Bork *et al*., 2010). In the present study, we detected telomere shortening, which is a symptom of senescence, during long-term culture of MSCs as reported previously (Bonab *et al*., 2006; Choi *et al*., 2010).

Recently, some studies have investigated DNA methylation of genes related to adipogenic differentiation and senescence in MSCs (Noer *et al*., 2006, 2007; Shibata *et al*., 2007). In a study by Noer *et al*. (2007), CpG methylation in the *LEP* promoter in MSCs from adipose tissue was changed due to senescence. Shibata *et al*. (2007) reported that promoter methylation of $p16^{INK4A}$, which is a tumor suppressor gene, was higher for early-passage MSCs than for late-passage MSCs, showing that careful observation of DNA methylation should be considered during long-term culture of MSCs. A significant difference in methylation between early-passage and late-passage MSCs has also recently been reported (Bork *et al*., 2010). However, epigenetic regulation, such as change of DNA methylation in MSCs upon long-term culture, remained to be investigated. We therefore profiled DNA methylation

to measure changes in the methylation patterns between early-passage and late-passage MSCs. Regarding greater than two-fold methylation differences for genes between early and late passages, more than 1,000 genes showed higher methylation at late passage than at early passage. In addition, genes exhibiting methylation differences between early and late passages were most located in LCPs, whereas no genes in HCPs were detected. Previous studies have reported that LCPs are not only associated with tissue-specific genes but also hypermethylated followed by down-regulation of genes, while genes containing HCPs are broadly expressed as well as hypomethylated (Elango and Yi, 2008; Rubinstein *et al*., 2010). The overall trend between methylation and CpG content in promoter of genes previously profiled by these research groups is consistent with our findings.

When comparing hypermethylated genes at both early and late passages, methylation tended to be lower in late passage than in early passage, which is a result opposite from that regarding methylation differences between early and late passages. In a study by Zhang *et al*. (2008) that evaluated global DNA methylation in HEFs using an immuno-fluorescence assay, the global DNA methylation pattern decreased gradually upon prolonged culture. Nilsson *et al*. (2005) also reported that the overall level of DNA methylation in growth plate chondrocytes decreased during growth plate senescence. In contrast, Bork *et al*. (2010) observed that except for some genes such as homeobox genes, methylation patterns were maintained throughout long-term culture of BM-MSCs, showing different results than those in our present study. A possible reason for the discrepancy between Bork *et al*. and our observations may be the use of different detection and analysis methods. However, based on previous studies (Nilsson *et al*., 2005; Zhang *et al*., 2008) and the results presented here, the decrease in DNA methylation upon long-term culture may contribute to replicative senescence in cells having a finite proliferative capacity.

In the GO analysis of genes with methylated promoters, genes related to cellular migration and morphogenesis or involved in differentiation were two times more methylated at late passage than at early passage. In addition, hypermethylated genes (methylation peak ≥ 2) were associated with transport and neuron differentiation and were hypermethylated at late passage. Considering that DNA methylation in part regulates gene silencing and that the differentiation potential of MSCs decreases at late passage (Suzuki and Bird, 2008; Choi *et al*., 2010), these results suggest that genes associated with differentiation may become methylated during long-term culture, leading to a decrease in differentiation potential.

There were more gene promoters hypermethylated at early passage than at late passage, suggesting that early-passage MSCs show more stable gene silencing through promoter methylation than do late-passage MSCs. We also observed hypermethylation of BAD, BCL-2, CASP7 and CASP9, which belong to the apoptosis-related pathway, at early passage. Considering that three of these genes induce apoptosis, this result implies that silencing through hypermethylation may promote cell survival in early-passage MSCs but not in late-passage cells. Genes such as GADD45B and TP73, which belong to the p53 signaling pathway that is responsible for replicative senescence through growth arrest (Beausejour *et al*., 2003), were also hypermethylated at early passage, compared with late passage, suggesting that transcription of these genes is in part regulated by DNA methylation in the promoter. In addition, genes regulating cell cycle (CDK2, CDK4 and PCNA) and genes regulating DNA replication (POLE, POLD4 and RFC2) were hypermethylated at late passage, compared with early passage. Therefore, it is plausible that the reduction in DNA replication and cell proliferation that causes MSC senescence is related to promoter DNA methylation of these regulatory genes.

Previous studies have shown that expression of genes related to differentiation as well as the adipogenic differentiation potential of MSCs decreases due to long-term culture (Digirolamo *et al*., 1999; Banfi *et al*., 2000; Noer *et al*., 2007). Noer *et al*. (2007) proposed the possibility of impairing up-regulation of LEP upon adipogenic stimulation in senescent MSCs due through changes in CpG methylation in the promoter, as previously mentioned. However, senescence did not induce changes in PPARG2, FABP4 and the LPL promoter CpG methylation. Interestingly in our study, adiponectin (ADIPOQ), which is a molecular marker for adipogenesis (Lara-Castro *et al*., 2007), was hypermethylated in late-passage cells, suggesting that its hypermethylation may in part be related to a decrease in adipogenic differentiation due to senescence. In the present study, we also showed that hypermethylated genes exhibited a decrease in mRNA expression, supporting this correlation between DNA methylation and gene expression.

MSC senescence leads to an alteration in miRNA expression (Wagner *et al*., 2008). Ibanez-Ventoso *et al*. (2006) reported that miRNA expression decreased during aging in Caenorhabditis elegans. These studies imply that changes in miRNA expression are closely associated with cellular senescence or aging; they also shed light on the mechanisms,

including genetic and epigenetic alterations that may affect miRNA expression. MiRNAs that were down-regulated in chronic lymphocytic leukemia compared with normal B-cells were methylated in their promoter regions, indicating that miRNA promoter methylation may be involved in transcriptional silencing of pri-miRNAs (Pallasch *et al*., 2009). In the present study, hypermethylation of has-miR-200c, which regulates BMI-1, a repressor of INK4a/ARF expression, and has-miR-210, which is induced as a cellular response to hypoxic stress (Crosby *et al*., 2009) in early-passage cells, decreased at late passage. In addition, has-miR-127, has-miR-130a, has-miR-136 and has-miR-150 were hypermethylated in early-passage cells, while has-miR-27b, has-miR-411 and has-miR-195 were hypermethylated at late-passage cells. Intriguingly, hypermethylated miRNAs increased at late passage as compared with early passage. Therefore, given an overall age-related decrease in miRNA expression (Liang *et al*., 2009) as well as the suppression of miRNA expression by methylation (Pallasch *et al*., 2009), it is possible that MSC senescence might induce the down-regulation of miRNAs through methylation.

In conclusion, we profiled the genome-scale DNA and miRNA promoter methylation patterns of MSCs between early and late passages. We observed that genes exhibiting methylation differences between early and late passages were most located in LCPs. In addition, there were more gene promoters hypermethylated at early passage than at late passage. Our data show that long-term culture of MSCs causes major changes in the methylation pattern in DNA promoters. These findings may help our understanding of the mechanisms regulating senescence-associated epigenetic modifications.

Methods

MSC culture

The human BM-derived MSCs purchased from Lonza (lot 7F3674, Walkersville, ML) were cultured in Dulbecco's Modified Eagle's Medium-low glucose (DMEM-LG; Invitrogen, Carlsbad, CA) containing 10% fetal bovine serum (Invitrogen, Carlsbad, CA) at 37°C in 5% CO_2. After the MSCs reached 80% confluency, cells were subcultured using 0.25% trypsin/EDTA (Invitrogen, Carlsbad, CA). Informed consent was obtained from Poietics human mesenchymal stem cell systems (Lonza, Walkersville, ML).

Analysis of relative telomere length

Genomic DNA was purified from the experimental samples (MSCs at P5, P7, P9, P12 and P15) and the reference NCCIT cells (human embryonic carcinoma cells; telomerase-positive cell line) using the Wizard® Genomic DNA Purification Kit (Promega, Madison, WI) as specified by the manufacturer. Relative telomere lengths were measured by quantitative real-time PCR amplification of telomere repeats (T) and the single-copy gene *36B4* (S) using the ABI 7500 Real-Time PCR System (Applied Biosystems, Foster City, CA). The *36B4* gene was used to normalize variations in DNA concentration across samples. The primers and thermal cycling profiles were adopted from Cawthon (Cawthon, 2002). T and S standard curves (i.e., Ct vs. log quantity) were generalized using serial dilutions of DNA ranging from 200 to 12.5 ng from NCCIT as described previously (Guillot *et al*., 2007). Ct values in experimental samples were determined from semi-log amplification plots, and the standard curve was used to determine the quantity of telomere repeats. Note that this latter quantity is equivalent to the level of dilution of the arbitrary reference NCCIT needed to yield the same number of PCR cycles during the exponential phase. Relative telomere length was estimated as the $T_{quantity}/S_{quantity}$ (T/S) ratio, which is proportional to the mean terminal restriction fragment telomere (TRF) length (Cawthon, 2002). The telomere and *36B4* PCRs were run on separate plates, and the standard curve was included in each run to allow relative quantification between samples of 50 ng per sample. The concentration of reagents was 25 μl of SYBR® Premix Ex Taq™ II (Takara BIO, Shiga, Japan) and 1 μl of ROX, with the following final primer concentrations: Tel 1, 270 nM; Tel 2, 900 nM; 36B4u, 300 nM; and 36B4d, 500 nM. The thermal cycling conditions were initiated at 95°C for 10 min; this step was followed by 40 cycles of 95°C for 15 s and then 54°C for 2 min for telomere PCR. This was followed by 40 cycles of 95°C for 15 s and then 58°C for 1 min for *36B4* PCR. The sequences of primers are listed in Supplemental Data Table S5.

MeDIP assay

The purification of genomic DNA from MSCs at P5 and P15 was performed using the Wizard® Genomic DNA Purification Kit (Promega, Madison, WI) as specified by the manufacturer. Before carrying out MeDIP, we sonicated genomic DNA to generate random fragments between 300 and 1,000 bp. Four μg of fragmented DNA was denatured for 10 min at 95°C and immunoprecipitated with 10 μl of monoclonal antibody against 5-methylcytidine (Calbiochem, SanDiego, CA) in a final volume of 500 μl IP buffer (10 mM sodium phosphate, pH 7.0, 140 mM NaCl, 0.05% Triton X-100) for 2 h at 4°C. After adding 40 μl of Dynabeads® M-280 Sheep anti-Mouse IgG (Dynal Biotech, Oslo, Norway) to the mixture, it was incubated for 2 h at 4°C and washed with 700 μl of IP buffer. Then the beads were collected, incubated with proteinase K for 3 h at 50°C, and then the methylated DNA was recovered by phenol-chloroform extraction followed by ethanol precipitation. To validate IEF, GPR109A, SFRS5 and PEX3 genes were amplified using PCR as previously described (Weber *et al*., 2007). The amplified products were evaluated by agarose gel electrophoresis. Primers used for MeDIP validation are listed in Supplemental Data Table S5.

Whole genome amplification of input and IEF

Whole genome amplification (WGA) of input and IP DNA from MSCs at P5 and P15 was performed using the GenomePlex WGA kit (Sigma, St. Louis, MO) according to the manufacturer's instructions. For OmniPlex library preparation, 10 μl of DNA solution (1 ng/μl of input or IEF) and 2 μl of 1× Library Stabilization Solution were mixed, incubated at 95°C for 2 min, and then added to 1 μl of Library Preparation Enzyme. The mixture was performed in a PCR iCycler (Bio-Rad, Richmond, CA) at 16°C for 20 min, 24°C for 20 min, 37°C for 20 min, and 75°C for 5 min, and then it was held at 4°C. For WGA, the mixture was added to 7.5 μl of 10× Amplification Master Mix, 47.5 μl of Nuclease-free water and 5 μl of WGA DNA polymerase. Then the mixture was denatured at 95°C for 3 min and then 40 cycles of 94°C for 15 s and 65°C for 5 min. The mixture was finally purified using the QIAquick PCR Purification Kit (Qiagen, Chatsworth, CA).

Hybridization of microarray

To examine the methylation pattern of genomic DNA at P5 and P15, two Human 2.1 M Deluxe Promoter Arrays (NimbleGen, Madison, WI) containing 28,266 CpG islands and 475 miRNA promoters were used. One μg of the amplified input and IEF DNA was separately labeled by Cy3-dCTP and Cy5-dCTP (GeneChem, Shanghai, China) using the BioPrime® Array CGH Genomic Labeling System (Invitrogen, Carlsbad, CA) according to the manufacturer's instructions. Twenty-one μl (1 μg) of input (or IEF) and 20 μl of 2.5× random primer solution were mixed and denatured at 95°C for 5 min. For labeling input and IEF DNA, 3 μl of Cy3- (or Cy5-) dCTP, 5 μl of 10× dCTP nucleotide mixture and 1 μl of Klenow fragment (exo-) were added to the denatured mixture. The mixture was incubated at 37°C for 2 h and then stopped with 5 μl of stop buffer. The labeled probes (Cy3-input and Cy5-IEF) were purified using the QIAquick PCR Purification Kit. The hybridization procedure was performed using the NimbleGen Hybrdization Kit according to the manufacturer's instructions. For hybridization, Cy3-input and Cy5-IEF were loaded on a Human 2.1M Deluxe Promoter Array (NimbleGen, Madison, WI), and then it was hybridized at 42°C for 20 h using the MAUI 12-Bay Hybridization System (BioMicro Systems, Salt Lake City, UT). The hybridized array was washed with Wash I, II and III and then spin-dried.

Microarray analysis

We scanned the arrays with an Axon 4000B scanner and analyzed them using the NimbleScan 2.5 (NimbleGen, Madison, WI) software package and Microsoft Excel. Features with poor signal-to-noise ratios or saturated pixels were excluded from further analysis. We calculated the ratio between Cy3 and Cy5 signals for all high-quality features and normalized the ratio using NimbleScan 2.5 optimized settings. Methylated find-peak analysis based on the permutation-based algorithm was used to identify statistically significant peaks in the scaled log2-ratio data, which are likely to indicate methylation events. This analysis estimated the false discovery rate (FDR) for each peak (Benjamini and Hochberg, 1995) by repeatedly and randomly permuting the log-ratio data and searching for peaks. Strong peaks were characterized by consecutive probes with positive log-ratio values and generally low corresponding FDRs (P-value < 0.01). The resulting methylation values of promoter CpG sites were expressed by log2-transformation; therefore, methylation values of 1 indicate that the methylation of input was equal to the methylation of IP DNA. Methylation levels at P5 and P15 MSCs were calculated.

The array data have been deposited in the Gene Expression Omnibus (GEO; http//www.ncbi.nlm.nih.gov/projects/geo/). The accession number for the data is GSE30018. The reviewer access link is http://www.ncbi.nlm.nih.gov/geo/info/linking.html.

Bioinformatics analyses

Human promoters could be classified into three categories to distinguish HCPs, LCPs and ICPs (Nelson and Nusse, 2004). We calculated CpG O/E in the promoter region, which is defined as 5 kp upstream to 1 kb downstream of the gene transcriptional start site as defined by NimbleGen. CpG O/E was calculated using the following formula: (CpG frequency)/(C frequency × G frequency). The three categories of promoters were defined: HCPs with CpG O/E above 0.75 and GC content (G and C frequency) above 55%; LCPs with a CpG O/E under 0.47; and remaining ICPs that were neither HCPs nor LCPs.

Functions of differentially methylated genes between P5 and P15 MSCs were determined using v6.7. The physiological function of regulated genes was analyzed using the pathway analysis and visualization tool (http://www.asgbioinformatics.wur.nl/) (Te Pas *et al.*, 2007).

Pathway analysis of genes in methylation peaks showing P-value scores more than two-fold meaning P-values (≤ 0.01) at P5 and P15 was performed using KEGG pathway database (http://www.genome.jp/kegg/pathway.html).

MSP

Sodium bisulfite modification of genomic DNA from MSCs at P5 and P15 was performed using MethylEasy™ DNA Bisulphite Modification Kit (Human Genetic Signatures, Randwick, Australia) as specified by the manufacturer. Twenty μl of genomic DNA (2,000 ng/μl) was bisulfite converted. This step leads to the deamination of non-methylated cytosines to uracils whereas methylated cytosines are not modified by bisulfite. After bisulfite modification, genomic DNA concentration was measured using e-spect ES-2 spectrophotometer (Malcom). Methylation changes of the CpGs of three gene promoters (SMAD9, CPEB1 and FEN1) were validated using MSP. The MSP primers were designed using MethPrimer software (available on the World Wide Web at http://www.urogene.org/methprimer/) and are listed in Supplemental Data Table S5. Three μl of bisulfite-modified DNA, 10 pmol of each MSP primer set, and 15 μl of EF-Taq Premix II (SolGent, Daejeon, Korea) were mixed with water to a final volume of 30 μl. The mixture was amplified by hot-start PCR (iCycler, Bio-Rad, Richmond, CA) as follows: 32 cycles of 1 min of denaturation at 94°C, 1 min of annealing at 56°C, and 1

min of elongation at 72°C. Ten μl of the PCR product was loaded onto a 10% polyacrylamide gel. The DNA was visualized by staining with EtBr.

RT-PCR

Total RNA extracted from MSCs at P5 and P15 was reverse-transcribed with SuperScript III reverse transcriptase (Invitrogen, Carlsbad, CA). The synthesized cDNA was mixed with 2× EF-Taq Premix II (SolGent, Daejeon, Korea), and gene-specific primers were synthesized by Genotech (Daejeon, Korea). The sequences of the primers (CPEB1, GMPPA, CDKN1A, TBX2, SMAD9, MCM2, MAML2, FEN1, CDK4 and β-actin) are listed in Supplemental Data Table S5. PCR was performed using Swift™ MaxPro Thermal Cycler (Esco, Oak Ridge, NJ). The amplification conditions consisted of an initial melt at 94°C for 4 min, followed by 22 to 35 cycles of denaturation at 94°C for 1 min, annealing at 60°C for 1 min, extension at 72°C for 1 min and final extension at 72°C for 10 min. The amplified products were evaluated by polyacrylamide gel electrophoresis.

Statistical analysis

The relative telomere length was expressed as the mean ± standard error of measurement (SEM) from three independent experiments. Statistical analysis was performed using SPSS 13.0 (SPSS Inc., Chicago, IL). The data were tested using a one-way ANOVA followed by post hoc testing with Tukey's honestly significant difference (HSD) test, and *P*-values < 0.05 were considered significant.

Supplemental data

Supplemental data include a figure and five tables and can be found with this article online at http://e-emm.or.kr/article/article_files/SP-44-8-05.pdf.

Acknowledgements

We want to thank GenoCheck Co. (Gyeonggi-do, Korea) for assistance in experiment of DNA methylation array. This research was supported by Basic Science Research Program through the National Research Foundation of Korea (NRF) funded by the Ministry of Education, Science and Technology (2010-0023808 to M.R.C.) and the National Research Foundation of Korea Grant funded by the Korean Government (No.2011-0030768 to Y.G.C.).

References

Antequera F. Structure, function and evolution of CpG island promoters. Cell Mol Life Sci 2003;60:1647-58

Banfi A, Muraglia A., Dozin B, Mastrogiacomo M, Cancedda R, Quarto R. Proliferation kinetics and differentiation potential of *ex vivo* expanded human bone marrow stromal cells: Implications for their use in cell therapy. Exp Hematol 2000;28:707-15

Baxter MA, Wynn RF, Jowitt SN, Wraith JE, Fairbairn LJ, Bellantuono I. Study of telomere length reveals rapid aging of human marrow stromal cells following *in vitro* expansion. Stem Cells 2004;22:675-82

Beausejour CM, Krtolica A, Galimi F, Narita M, Lowe SW, Yaswen P, Campisi J. Reversal of human cellular senescence: roles of the p53 and p16 pathways. EMBO J 2003;22:4212-22

Benjamini Y, Hochberg Y. Controlling the false discovery rate: a practical and powerful approach to multiple testing. J R Statist Soc B 1995;57:289-300

Bernardo ME, Zaffaroni N, Novara F, Cometa AM, Avanzini MA, Moretta A, Montagna D, Maccario R, Villa R, Daidone MG, Zuffardi O, Locatelli F. Human bone marrow derived mesenchymal stem cells do not undergo transformation after long-term *in vitro* culture and do not exhibit telomere maintenance mechanisms. Cancer Res 2007;67:9142-9

Bird A. DNA methylation patterns and epigenetic memory. Genes Dev 2002;16:6-21

Bonab MM, Alimoghaddam K, Talebian F, Ghaffari SH, Ghavamzadeh A, Nikbin B. Aging of mesenchymal stem cell *in vitro*. BMC Cell Biol 2006;7:14

Bork S, Pfister S, Witt H, Horn P, Korn B, Ho AD, Wagner W. DNA methylation pattern changes upon long-term culture and aging of human mesenchymal stromal cells. Aging Cell 2010;9:54-63

Bruder SP, Jaiswal N, Haynesworth SE. Growth kinetics, self-renewal, and the osteogenic potential of purified human mesenchymal stem cells during extensive subcultivation and following cryopreservation. J Cell Biochem 1997;64:278-94

Cawthon RM. Telomere measurement by quantitative PCR. Nucleic Acids Res 2002;30:e47

Choi MR, Kim HY, Park JY, Lee TY, Baik CS, Chai YG, Jung KH, Park KS, Roh W, Kim KS, Kim SH. Selection of optimal passage of bone marrow-derived mesenchymal stem cells for stem cell therapy in patients with amyotrophic lateral sclerosis. Neurosci Lett 2010;472:94-8

Crosby ME, Kulshreshtha R, Ivan M, Glazer PM. MicroRNA regulation of DNA repair gene expression in hypoxic stress. Cancer Res 2009;69:1221-9

Dahl JA, Duggal S, Coulston N, Millar D, Melki J, Shahdadfar A, Brinchmann JE, Collas P. Genetic and epigenetic instability of human bone marrow mesenchymal stem cells expanded in autologous serum or fetal bovine serum. Int J Dev Biol 2008;52:1033-42

Digirolamo CM, Stokes D, Colter D, Phinney DG, Class R, Prockop DJ. Propagation and senescence of human marrow stromal cells in culture: a simple colony-forming assay identifies samples with the greatest potential to propagate and differentiate. Br J Haematol 1999;107:275-81

Elango N, Yi SV. DNA methylation and structural and functional bimodality of vertebrate promoters. Mol Biol Evol 2008;25:1602-8

Godlewski J, Newton HB, Chiocca EA, Lawler SE. MicroRNAs and glioblastoma; the stem cell connection. Cell Death Differ 2010;17:221-8

Guillot PV, Gotherstrom C, Chan J, Kurata H, Fisk NM. Human first-trimester fetal MSC express pluripotency markers and grow faster and have longer telomeres than adult MSC. Stem Cells 2007;25:646-54

Hammond SM, Sharpless NE. HMGA2, microRNAs, and stem cell aging. Cell 2008;135:1013-6

Ibanez-Ventoso C, Yang M, Guo S, Robins H, Padgett RW, Driscoll M. Modulated microRNA expression during adult lifespan in Caenorhabditis elegans. Aging Cell 2006;5: 235-46

Lara-Castro C, Fu Y, Chung BH, Garvey WT. Adiponectin and the metabolic syndrome: mechanisms mediating risk for metabolic and cardiovascular disease. Curr Opin Lipidol 2007;18:263-70

Liang R, Bates DJ, Wang E. Epigenetic control of microRNA expression and aging. Curr Genomics 2009;10:184-93

Nelson WJ, Nusse R. Convergence of Wnt, beta-catenin, and cadherin pathways. Science 2004;303:1483-7

Nilsson O, Mitchum RD Jr, Schrier L, Ferns SP, Barnes KM, Troendle JF, Baron J. Growth plate senescence is associated with loss of DNA methylation. J Endocrinol 2005;186:241-9

Noer A, Sorensen AL, Boquest AC, Collas P. Stable CpG hypomethylation of adipogenic promoters in freshly isolated, cultured, and differentiated mesenchymal stem cells from adipose tissue. Mol Biol Cell 2006;17:3543-56

Noer A, Boquest AC, Collas P. Dynamics of adipogenic promoter DNA methylation during clonal culture of human adipose stem cells to senescence. BMC Cell Biol 2007;8:18

Pallasch CP, Patz M, Park YJ, Hagist S, Eggle D, Claus R, Debey-Pascher S, Schulz A, Frenzel LP, Claasen J, Kutsch N, Krause G, Mayr C, Rosenwald A, Plass C, Schultze JL, Hallek M, Wendtner CM. miRNA deregulation by epigenetic silencing disrupts suppression of the oncogene PLAG1 in chronic lymphocytic leukemia. Blood 2009;114:3255-64

Rombouts WJ, Ploemacher RE. Primary murine MSC show highly efficient homing to the bone marrow but lose homing ability following culture. Leukemia 2003;17:160-70

Rubinstein JC, Tran N, Ma S, Halaban R, Krauthammer M. Genome-wide methylation and expression profiling identifies promoter characteristics affecting demethylation-induced gene up-regulation in melanoma. BMC Med Genomics 2010;3:4

Schaefer A, Jung M, Miller K, Lein M, Kristiansen G, Erbersdobler A, Jung K. Suitable reference genes for relative quantification of miRNA expression in prostate cancer. Exp Mol Med 2010;42:749-58

Shibata KR, Aoyama T, Shima Y, Fukiage K, Otsuka S, Furu M, Kohno Y, Ito K, Fujibayashi S, Neo M, Nakayama T, Nakamura T, Toguchida J. Expression of the p16INK4A gene is associated closely with senescence of human mesenchymal stem cells and is potentially silenced by DNA methylation during *in vitro* expansion. Stem Cells 2007;25: 2371-82

Sinkkonen L, Hugenschmidt T, Berninger P, Gaidatzis D, Mohn F, Artus-Revel CG, Zavolan M, Svoboda P, Filipowicz W. MicroRNAs control de novo DNA methylation through regulation of transcriptional repressors in mouse embryonic stem cells. Nat Struct Mol Biol 2008;15:259-67

Suzuki MM, Bird A. DNA methylation landscapes: provocative insights from epigenomics. Nat Rev Genet 2008;9:465-76

Te Pas MF, Hulsegge I, Coster A, Pool MH, Heuven HH, Janss LL. Biochemical pathways analysis of microarray results: regulation of myogenesis in pigs. BMC Dev Biol 2007;7:66

Wagner W, Horn P, Castoldi M, Diehlmann A, Bork S, Saffrich R, Benes V, Blake J, Pfister S, Eckstein V, Ho AD. Replicative senescence of mesenchymal stem cells: a continuous and organized process. PLoS One 2008;3:e2213

Weber M, Hellmann I, Stadler MB, Ramos L, Paabo S, Rebhan M, Schubeler D. Distribution, silencing potential and evolutionary impact of promoter DNA methylation in the human genome. Nat Genet 2007;39:457-66

Zhang W, Ji W, Yang J, Yang L, Chen W, Zhuang Z. Comparison of global DNA methylation profiles in replicative versus premature senescence. Life Sci 2008;83:475-80